Low-temperature synthesis of rhodium phosphide on alumina and investigation of its catalytic activity toward the hydrodesulfurization of thiophene

doi: info:doi/10.1016/j.apcata.2016.01.040

Low-temperature synthesis of rhodium phosphide on alumina and investigation of its catalytic activity toward the hydrodesulfurization of thiophene

Yasuharu Kanda[a*], Yuki Matsukura[b], Ayaka Sawada[c], Masatoshi Sugioka[d], and Yoshio Uemichi[a]

[a]Applied Chemistry Research Unit, College of Environmental Technology, Graduate School of Engineering, Muroran Institute of Technology, 27-1 Mizumoto, Muroran 050-8585, Japan

[b]Division of Applied Sciences, Graduate School of Engineering, Muroran Institute of Technology, 27-1 Mizumoto, Muroran 050-8585, Japan

[c]Division of Chemical and Materials Engineering, Graduate School of Engineering, Muroran Institute of Technology, 27-1 Mizumoto, Muroran 050-8585, Japan

[d]Aeronautics and Astronautics Unit, College of Design and Manufacturing Technology, Graduate School of Engineering, Muroran Institute of Technology, 27-1 Mizumoto, Muroran 050-8585, Japan

Abstract

In this study, the low-temperature synthesis of rhodium phosphide (Rh_2P) on alumina (Al_2O_3) using triphenylphosphine (TPP) as a phosphorus (P) source and its catalytic activity toward

hydrodesulfurization (HDS) were investigated to prepare a highly active HDS catalyst. TPP was more easily reduced than phosphate, and Rh_2P was formed in the P(T)/Rh/Al_2O_3 catalyst prepared from TTP at lower temperature as compared with the temperature required by Rh-P(A)/Al_2O_3 catalyst prepared from a phosphate precursor. However, after reduction at a low temperature (450 °C), excess P covered the surface of Rh_2P. The optimal reduction temperature for HDS rate of the P(T)/Rh/Al_2O_3 catalyst (650 °C) was lower than that of the Rh-P(A)/Al_2O_3 catalyst (800 °C). Furthermore, this temperature was slightly higher than the optimal reduction temperature for CO uptake (600 °C). These results are explained as follows: HDS rate is increased by both elimination of excess P on the active sites at higher reduction temperatures and enhancement of the crystallinity of Rh_2P. Furthermore, because the particle size of the P(T)/Rh/Al_2O_3 catalyst (ca. 1.2 nm) was substantially smaller than that of the Rh-P(A)/Al_2O_3 catalyst, the P(T)/Rh/Al_2O_3 catalyst exhibited greater HDS rate compared with the Rh-P(A)/Al_2O_3 catalyst.

Keywords

Rhodium phosphide catalyst; Alumina support; Hydrodesulfurization; Triphenylphosphine; Low-temperature synthesis

1. Introduction

Recently, the petroleum industry has claimed that the development of highly active hydrodesulfurization (HDS) catalysts that exhibit greater activity than commercial CoMo catalysts will prevent air pollution, acid rain, and the deactivation of automotive exhaust catalysts [1-3]. New active phases, especially nickel phosphide (Ni_2P), have received extensive attention [2-22]. Furthermore, our group [23-27] and Bussell's group [3, 28] reported that rhodium phosphide (Rh_2P) supported on SiO_2 exhibits high and stable catalytic activity toward the HDS reaction.

Phosphate reduction is a convenient and simple method to prepare phosphide catalysts [16]. Because phosphate has strong P–O bonds, phosphate reduction requires high temperatures [3]. In general, SiO_2, which does not strongly interact with phosphate, is a suitable support for phosphide catalysts [2, 3, 10, 11]. For industrial usage, Al_2O_3 is a suitable support because it exhibits greater mechanical strength and

stability than SiO_2. Unfortunately, Al_2O_3 is not a suitable support for phosphide catalysts, because phosphate reacts with Al_2O_3 to form $AlPO_4$ [3, 6, 10, 11]. In fact, we have reported that the optimal reduction temperature (800 °C) for HDS activity of the Rh-P/Al_2O_3 catalyst is remarkably higher than that for HDS activity of the Rh-P/SiO_2 catalyst (550 °C) and that this higher temperature induces aggregation of Rh_2P [24, 27]. Therefore, we expect that high HDS activity can be obtained via the low-temperature synthesis of highly dispersed Rh_2P on an Al_2O_3 support.

Numerous reports have described the synthesis of phosphide catalysts at low temperatures. Teixeira da Silva et al. reported that the formation temperature of Ni_2P, which was prepared from a phosphate precursor, can be decreased by the addition of Pd [29]. Previously, we reported that the reduction temperature of phosphates on Al_2O_3 and SiO_2 substrates and the formation temperatures of Rh_2P were decreased by the addition of Na [30]. However, noble metal addition is not an appropriate method for the synthesis of noble metal phosphides, and added Na would decrease the catalytic activity. Thus, phosphite, which is more reducible than phosphate, has been used as a P precursor to form noble metal phosphides

[31]. However, phosphite on an Al_2O_3 support is less reducible than that on other supports [32]. Some P precursors without oxygen, such as phosphine (PH_3) and trioctylphosphine (TOP), have been reported [3, 12, 33, 34]. PH_3 easily reacts with metals to form phosphides at low temperatures; however, this reagent is highly toxic. TOP also reacts with metal precursors such as acetylacetonate complexes to form phosphides at lower temperatures. But this method requires a large amount of a P precursor. Furthermore, the washed phosphides were impregnated into Al_2O_3 to obtain the supported catalyst [35], which is a complicated method. On the other hand, some reports described synthesis of Ni_2P catalyst using triphenylphosphine ($(C_6H_5)_3P$, TPP) [36, 37], but this method was also carried out in trioctylamine solution under N_2 flow.

In our previous paper, we reported that rhodium and palladium phosphides were more easily formed using TPP compared with the corresponding phosphides prepared from phosphate, even in cases where the phosphides prepared from phosphate were calcined [25]. TPP is widely used as a ligand for homogeneous noble metal catalysts, indicating that TPP preferentially adsorbs onto noble metals rather than onto the

supporting substrates. In addition, we observed that the phosphates that interacted with noble metals were more easily reduced than those on supports [26]. We expect that Rh_2P would easily form on Al_2O_3 when TPP is used as a P precursor. In this study, the low-temperature synthesis of Rh_2P on Al_2O_3 using TPP was examined to enhance the HDS activity of this phosphide-based catalyst.

2. Experimental

2.1. Catalyst preparation

Alumina (Al_2O_3, BET surface area 101 $m^2\ g^{-1}$) was supplied by Nippon Aerosil Co. The Rh/Al_2O_3 was prepared using an impregnation method. Rhodium (III) chloride trihydrate ($RhCl_3 \cdot 3H_2O$, Kanto Chemical Co.) was used as an Rh precursor and was dissolved in water. The Rh loading was 5 or 10 wt%. After impregnation, the Rh/Al_2O_3 was dried at 110 °C for 24 h, followed by heat treatment under an N_2 stream at 450 °C for 1 h to decompose the Rh salt. The ramp rate for the N_2 treatment was 10 °C min^{-1}.

The TPP-added Rh/Al_2O_3 ($P(T)/Rh/Al_2O_3$) catalyst was also prepared

by an impregnation method. A TPP hexane solution was impregnated into Rh/Al_2O_3. The P loading was 1.5 or 3 wt%, and the P/Rh molar ratio in the catalysts was 1.0. The $P(T)/Rh/Al_2O_3$ catalyst was dried under an N_2 stream at 110 °C for 24 h to avoid oxidation of TPP. After drying, the catalyst was sieved into 30- to 42-mesh-size granules. The high-loading (Rh: 10 wt%, P: 3 wt%) catalyst was labeled as $HL\text{-}P(T)/Rh/Al_2O_3$.

2.2. Catalyst characterization

The $P(T)/Rh/Al_2O_3$ catalyst was characterized using temperature-programmed reduction (TPR), X-ray diffraction (XRD), X-ray photoelectron spectroscopy (XPS), transmission electron microscopy (TEM), and carbon monoxide (CO) adsorption analyses. TPR measurements were performed using a Shimadzu GC-8A gas chromatograph. The catalyst (0.1 g) was heated in a He stream (30 ml min^{-1}) from room temperature to 110 °C at 10 °C min^{-1}, followed by He treatment at 110 °C for 1 h. After this He treatment, the catalyst was cooled to 30 °C in a He stream, and the He was switched to a hydrogen–nitrogen (5 vol% H_2 in N_2) gas mixture at 30 °C for 0.5 h before the measurement. The TPR profile was recorded as the temperature was

increased from 30 °C to 850 °C at 10 °C min^{-1}; a thermal conductivity detector (TCD) and a flame ionization detector (FID) were used to monitor the H_2 consumption and the formation of hydrocarbons, respectively. When a TPR profile was recorded by TCD, water was removed using a molecular sieve trap. XPS spectra of the catalysts after reduction were measured using a JEOL JPS-9010MX with Mg Kα radiation (10 kV, 5 mA). Binding energy of measured spectra were corrected using C 1s peak at 285.0 eV. The XRD patterns of the catalysts were collected using a Rigaku MiniFlex equipped with a Cu-Kα radiation source operated at 30 kV and 15 mA. TEM observations were carried out using a JEOL JEM-2100F. The conditions of TEM operation were an acceleration voltage of 200 kV and a magnification of 600000x. The particle size distribution and average particle size were determined from the measurements of 1000 particles in the TEM micrographs. The CO uptake of the P(T)/Rh/Al_2O_3 catalysts was measured using the pulse method. The P(T)/Rh/Al_2O_3 catalyst (0.1 g) was reduced under H_2 at 450 °C–750 °C for 1 h. CO was injected into the catalyst layer at 25 °C using a sampling loop (1.0 ml). The CO uptake was measured with a

Shimadzu GC-8A gas chromatograph equipped with a TCD.

2.3. Hydrodesulfurization of thiophene

The HDS of thiophene was performed at 350 °C under 0.1 MPa using a conventional fixed-bed flow reactor. The P(T)/Rh/Al_2O_3 catalyst (0.1 g) was charged into the quartz reactor and heated (10 °C min^{-1}) under an H_2 stream (30 ml min^{-1}) at 450 °C–700 °C for 1 h. A hydrogen–thiophene gas mixture (H_2/C_4H_4S molar ratio = 30), obtained by passing an H_2 stream through a thiophene trap cooled at 0 °C, was then introduced into the reactor (W/F = 37.9 g h mol^{-1}). The reaction products were analyzed using a gas chromatograph equipped with a FID and silicone DC-550 (length: 2 m, temperature: 110 °C) and Al_2O_3/KCl plot (ID: 0.53 mm, length: 25 m, film thickness: 10 μm, temperature: 60 °C–190 °C, rate: 7.5 °C min^{-1}) columns.

The HDS rate constant was calculated from the following equation under the assumption of a pseudo-first-order reaction:

$$k_{HDS} = \frac{-\ln(1-x/100)}{W/F} \quad (1)$$

where k_{HDS} is the reaction rate of thiophene HDS (mol h^{-1} g^{-1}) and x is the conversion at 3 h (%).

The turnover frequency (TOF) was calculated from the following equation:

$$TOF = \frac{Fx/100}{WA} \quad (2)$$

where F is the flow rate of thiophene (mol h^{-1}), W is the weight of catalyst loading (g), and A is the CO uptake (mol g^{-1}).

3. Results and Discussion

3.1. Low-temperature synthesis of Rh_2P on Al_2O_3 supports

We have reported that the reduction temperature strongly affects the formation of Rh_2P catalysts [23-27]. Therefore, the TPR profiles of the P(T)/Rh/Al_2O_3 catalyst were examined to clarify the reducibility of the rhodium oxide and TPP. **Figure 1** shows the TPR profile of the P(T)/Rh/Al_2O_3 catalyst recorded by TCD and FID. Some peaks (at 120 °C, 180 °C, 225 °C, and 490 °C) appeared in the TPR profile recorded by TCD. In the TPR profile recorded by FID, peaks appeared at 165 °C and 230 °C, indicating that these peaks were attributable to the formation of hydrocarbons such as benzene and cyclohexane. However, no peaks were observed at 120 °C and 490 °C in this profile. Hwang et al. reported that

rhodium oxide interacting with Al_2O_3 was reduced at 120 °C [38]. This result indicates that the peak at 120 °C was attributed to reduction of rhodium oxide interacted with Al_2O_3. Oyama et al. reported that the peak of phosphine (PH_3) production appeared around 530 °C (800 K) in the TPR profile of Ni_2P/SiO_2 precursor [7]. On the basis of these results, the peak at 490 °C is attributed to PH_3 formation.

In the TPR profile of the Rh-P/Al_2O_3 catalyst prepared from ammonium dihydrogen phosphate (Rh-P(A)/Al_2O_3), the hydrogen consumption, which was due to the reduction of $AlPO_4$, was observed above 700 °C. In contrast, the reduction peak of TPP appeared at remarkably lower temperatures (approximately 200 °C) compared with that of $AlPO_4$. Therefore, Rh_2P would be easily formed on Al_2O_3 when TPP is used as a P source. **Figure 2** shows the XRD patterns of P(T)/Rh/Al_2O_3 catalysts after reduction. Irrespective of the reduction temperature, no peaks associated with Rh species were observed in the XRD patterns, indicating that Rh species were highly dispersed on the Al_2O_3 support. Thus, we prepared the HL-P(T)/Rh/Al_2O_3 catalyst (Rh: 10 wt%, P: 3 wt%) to evaluate the formation of Rh_2P.

The TPR profile of the HL-P(T)/Rh/Al_2O_3 catalyst is shown in **Fig. 3**. Peaks were observed at the same temperatures as those of the P(T)/Rh/Al_2O_3 catalyst (standard loading). This similarity indicates that loading does not affect the reducibility of the Rh and P species. Therefore, Rh_2P formation over Al_2O_3 support can be evaluated using the XRD patterns of the HL-P(T)/Rh/Al_2O_3 catalyst. The XRD patterns of the high-loading catalyst reduced at various temperatures are shown in **Fig. 4**. Furthermore, **Fig. S1** shows the background (support) subtracted XRD patterns of the HL-P(T)/Rh/Al_2O_3 catalyst. After reduction at 350 °C, a broad peak for metallic Rh appeared around 41°. Furthermore, small peak also appeared at 47.2° and this peak would contain two peaks (Rh_2P: 46.7° and Rh: 47.8°). However, no peak for Rh_2P was observed at 32.6°. These results indicate that metallic Rh cores covered with Rh_2P shells would be formed. Above 450 °C, the intensity of the Rh_2P peaks increased, and that of the Rh peaks decreased. Moreover, the peak around 41° was hardly observed after reduction above 550 °C. Thus, Rh_2P would be completely formed on Al_2O_3 support by reduction with H_2 at 550 °C.

In the case of the XRD pattern of the Rh-P(A)/Al_2O_3 catalyst, peaks for

Rh_2P were observed after the catalyst was reduced at temperatures above 750 °C [24, 27]. Thus, the formation temperature of Rh_2P can be remarkably decreased through the use of TPP as a P source.

3.2. Surface properties and particle size of Rh_2P on Al_2O_3

Figure 5 shows the XPS spectra of P(T)/Rh/Al_2O_3 catalyst after reduction. After reduction at any temperature, the peak for Rh $3d_{5/2}$ appeared around 307.6 eV. Prins and Bussell reported that unsupported Rh_2P is metallic, which is consistent with observations for some other metal-rich phosphide phases (Ni_2P, Ni_3P, Cu_3P) [3, 28]. Furthermore, Rh 3d5/2 peak at 307.6 eV can be attributed to $Rh^{\delta+}$ [28]. Therefore, Rh in the P(T)/Rh/Al_2O_3 catalyst bears a partial positive charge. However, in the spectra of Rh-P(A)/Al_2O_3 catalyst reduced at 600 °C and 800 °C (**Fig. S2**), the peak for Rh $3d_{5/2}$ was observed at lower binding energy (307.4 and 307.2 eV) than that in the spectra of P(T)/Rh/Al_2O_3 catalyst after reduction (307.6 eV). The binding energy of metallic Rh species appears at 307.0-307.2 eV [39, 40]. Thus, Rh in the P(T)/Rh/Al_2O_3 catalyst after reduction is more cationic than that in the Rh-P(A)/Al_2O_3 catalyst. In the

XPS spectra of P(T)/Rh/Al_2O_3 and Rh-P(A)/Al_2O_3 catalysts after reduction, the peaks for P $2p_{3/2}$ were observed around 134.2-134.4 eV, which was attributed to phosphate species formed by exposing in air after reduction [28].

Table 1 shows the effect of the reduction temperature of P(T)/Rh/Al_2O_3 catalysts on their CO uptake. The maximum CO uptake was obtained in the case of the sample reduced at 600 °C. In the TPR profiles of the P(T)/Rh/Al_2O_3 catalyst recorded by TCD and FID (**Fig. 1**), the peak corresponding to PH_3 formation was observed at 490 °C. These results indicate the following: At lower reduction temperatures (below 450 °C), excess P (P/Rh = 1.0) covers exposed Rh sites on Rh_2P. In the TPR profile, hydrogen consumption peak for PH_3 formation was observed at 490 °C, as shown in Fig. 1. Because excess P adsorbed onto Rh_2P reacts with H_2 to form PH_3, CO uptake increased with increasing reduction temperature, when the reduction temperature was less than 600 °C. At reduction temperatures above 600 °C, the CO uptake gradually decreased with increasing temperature.

TEM images of the P(T)/Rh/Al_2O_3 catalysts after reduction are shown

in **Fig. 6**. Highly dispersed particles are evident in all of the micrographs. The particle size of the Rh species appeared to remain unchanged after reduction at 650 °C. **Figure 7** shows the particle size distribution of P(T)/Rh/Al_2O_3 catalysts after reduction, as calculated from TEM images. With increasing reduction temperature, the particle size distribution shifted to larger particle diameters. The particle distribution for the P(T)/Rh/Al_2O_3 catalyst before reduction exhibited a substantially sharp peak compared to that for the Rh-P(A)/Al_2O_3 catalyst (**Fig. S3**). The average particle size slightly increased with increasing reduction temperature (**Table 1**). Therefore, decrease of CO uptake above 600 °C can be explained by sintering of Rh_2P particles. Before reduction, the average particle size of the P(T)/Rh/Al_2O_3 catalyst (0.97 nm) was smaller than that of the Rh-P(A)/Al_2O_3 catalyst (2.60 nm, **Fig. S3**). Furthermore, the crystallite size of the Rh-P(A)/Al_2O_3 catalyst after reduction at 750 °C–850 °C was 5.3–8.5 nm (as calculated from its XRD pattern using the Scherrer equation) [24]. These results indicate that the particle size of the P(T)/Rh/Al_2O_3 catalyst was remarkably smaller than that of the Rh-P(A)/Al_2O_3 catalyst. After impregnation, $RhCl_3$ reacted with Al-OH to

form Rh^{3+}–O–Al species [41]. However, phosphate preferentially reacts with Al_2O_3 to form $AlPO_4$ [3, 6, 10, 11], resulting in the Rh species not interacting with the Al_2O_3 surface. Furthermore, when phosphate was used as a P source, the particle size of the Rh species increased with increasing P loading [26]. On the basis of these results, highly dispersed Rh_2P particles can be obtained by sequential impregnation using TPP as a P source.

3.3. Hydrodesulfurization of thiophene over the P(T)/Rh/Al_2O_3 catalyst

Figure 8 shows the HDS of thiophene over P(T)/Rh/Al_2O_3 catalyst reduced at 450-700 °C. In the P(T)/Rh/Al_2O_3 catalysts after reduction at lower temperatures (below 550 °C), the HDS conversion decreased with time on stream. On the other hand, the P(T)/Rh/Al_2O_3 catalysts reduced at higher temperatures (above 600 °C) showed stable HDS conversion. This stability was the same as that of Rh-P(A)/Al_2O_3 catalyst reduced at higher temperature (800 °C), as shown in **Fig. S4**.

The effect of reduction temperature on the HDS rate (k_{HDS}) of the

P(T)/Rh/Al_2O_3 catalyst after reaction for 3 h are listed in **Table 2**. The HDS rate of the catalyst remarkably increased as the reduction temperature was increased to 650 °C. In our papers, it was found that Rh_2P formation enhances HDS activity of Rh-P catalyst [23-27, 30]. After reduction at 450 °C, Rh_2P were observed in the XRD pattern of the P(T)/Rh/Al_2O_3 catalyst (**Figs. 4 and S1**). Furthermore, CO uptake increased with increasing reduction temperature from 450 °C to 600 °C, as shown in **Table 1**. Therefore, the enhancement of k_{HDS} can be explained by Rh_2P formation and elimination of excess P on Rh_2P. However, the optimal reduction temperature for maximum k_{HDS} was 650 °C, which is slightly higher than the temperature corresponding to maximum CO uptake (**Table 1**). In the XPS spectra, binding energy of Rh $3d_{5/2}$ hardly changed with increasing reduction temperature from 450 °C to 650 °C, as shown in **Fig. 5**. These results indicate that the difference in the optimal reduction temperatures for k_{HDS} and CO uptake cannot be explained by the electric state of Rh. In the case of the RuS_2/Al_2O_3 catalyst, pyrite-structured RuS_2 exhibited higher catalytic activity than amorphous RuS_2 for thiophene HDS [42]. Recently, it has been reported that particle

size strongly affects the crystallinity of Pt nanoparticles [43]. The disordered Rh particle habit persists to 4–5 nm; this value is substantially greater than that for Pt particles (2–3 nm) [44]. In the present study, because the particle size of Rh_2P on Al_2O_3 (after reduction at 450 °C) was ca. 1.2 nm (**Table 1**), the P(T)/Rh/Al_2O_3 catalyst should contain amorphous and/or low-crystallinity Rh_2P particles. When the reduction temperature exceeded 600 °C, even though the CO uptake decreased, the crystallinity of Rh_2P increased. Because the crystallinity of Rh_2P affects HDS activity and stability, the optimal reduction temperature for k_{HDS} was higher than that for CO uptake.

The maximum k_{HDS} of P(T)/Rh/Al_2O_3 catalyst (38.5 mmol g^{-1} h^{-1}) was 1.8 times higher than that of Rh-P(A)/Al_2O_3 catalyst (20.9 mmol g^{-1} h^{-1}, **Table S1**). High activity of the P(T)/Rh/Al_2O_3 catalyst can be explained by formation of highly dispersed Rh_2P particles using TPP as a P source. The optimal reduction temperature for maximum k_{HDS} of the P(T)/Rh/Al_2O_3 catalyst (650 °C) was 150 °C lower than that for maximum k_{HDS} of the Rh-P(A)/Al_2O_3 catalyst (800 °C) [24, 27]. This result is explained by Rh_2P being formed at a lower reduction temperature when

TPP is used as the P source. At temperatures above 650 °C, the HDS rate of the P(T)/Rh/Al_2O_3 catalyst decreased. The average particle size of the P(T)/Rh/Al_2O_3 catalyst slightly increased with increasing reduction temperature, as shown in **Table 1**. Thus, the decrease of HDS rate was due to sintering of Rh_2P particles.

The HDS reaction products were butanes, butenes, tetrahydrothiophene (THT), and trace amounts of cracking products. The selectivities for these reaction products in the thiophene HDS reaction over the P(T)/Rh/Al_2O_3 catalyst is listed in **Table 2**. Because the selectivities depend on the thiophene conversion rate, the product selectivities should be evaluated at similar thiophene conversion rates. At higher reduction temperatures (above 600 °C), the same thiophene conversion rate was obtained. The selectivity for THT increased with increasing reduction temperature. At similar conversion rates (ca. 53%), the P(T)/Rh/Al_2O_3 catalyst (reduced at 600 °C) exhibited remarkably higher butane selectivity and lower THT selectivity compared to those obtained with the Rh-P(A)/Al_2O_3 catalyst reduced at 800 °C (**Table S2**). TEM observations revealed that average particle size of P(T)/Rh/Al_2O_3 catalyst increased with increasing

reduction temperature. However, these particle sizes (**Table 1**) were remarkably smaller than that in the Rh-P(A)/Al_2O_3 catalyst (**Fig. S3**). These results indicate that small Rh_2P particles exhibit higher hydrogenation and C–S bond-cleavage abilities than larger particles. The selectivity of THT over Rh-P/SiO_2 catalyst increased with decreasing W/F [26]. Furthermore, the Rh_2P/SiO_2 catalyst strongly favored hydrogenation pathway [28]. Therefore, thiophene mainly reacts via hydrogenation route over the P(T)/Rh/Al_2O_3 catalyst with small Rh_2P particle.

3.4. Turnover frequency of the P(T)/Rh/Al_2O_3 catalyst

Table 2 also shows the turnover frequency (TOF) of the P(T)/Rh/Al_2O_3 catalysts reduced at various temperatures, which were calculated from CO uptake (assuming CO/Rh = 1). The TOFs of the P(T)/Rh/Al_2O_3 catalysts, which were significantly greater than that of the Rh/Al_2O_3 catalyst (15.9 h^{-1}, **Table S1**), increased as the reduction temperature was increased from 450 °C to 650 °C. These results imply that the formation and crystallinity of Rh_2P positively affected the TOF. However, the TOF of the P(T)/Rh/Al_2O_3 catalyst reduced at 650 °C (113.2 h^{-1}) was substantially

lower than that of the Rh-P(A)/Al_2O_3 catalyst (271.9 h^{-1}, **Table S1**). The XPS results (**Figs. 4 and S1**) revealed that the state of Rh in the P(T)/Rh/Al_2O_3 catalyst is more cationic than that of Rh-P(A)/Al_2O_3 catalyst. Furthermore, small Rh_2P particles in the P(T)/Rh/Al_2O_3 catalyst would be amorphous and/or poorly crystalline, as described above. Thus, the low TOF of the P(T)/Rh/Al_2O_3 catalyst is explained by the existence of cationic and/or low crystalline Rh_2P particles. In the HDS of thiophene at 370 °C, the Ni_2P/SiO_2 (P/Ni = 0.8) catalyst exhibited a TOF of 61 h^{-1} (0.017 s^{-1}) [19]. The TOF of the P(T)/Rh/Al_2O_3 catalyst reduced at 650 °C (113.2 h^{-1}) was higher than that of the Ni_2P/SiO_2 catalyst.

4. Conclusions

The low-temperature synthesis of Rh_2P using TPP as a P source and its catalytic activity toward the HDS reaction were investigated. Because TPP was easily reduced under H_2, Rh_2P was formed on Al_2O_3 supports at lower temperatures than Rh_2P formed from a phosphate precursor. The characterization results revealed the following: After reduction at lower temperature (below 450 °C), excess P covered the surface of Rh_2P. When

the reduction temperature was increased to 600 °C, excess P covering Rh_2P surface were reduced to the active Rh_2P phase. Furthermore, the average particle size of Rh_2P prepared from TPP was approximately 1.2 nm; this particle size was remarkably smaller than that of Rh_2P prepared from phosphate. The P(T)/Rh/Al_2O_3 catalyst exhibited maximal k_{HDS} after reduction at 650 °C, and this activity was 1.8 times higher than that of the Rh-P(A)/Al_2O_3 catalyst reduced at 800 °C. Thus, the high HDS rate of the P(T)/Rh/Al_2O_3 catalyst was caused by small Rh_2P particles formed at lower reduction temperatures.

Acknowledgment

We would like to thank Nippon Aerosil Co. for supplying the alumina support.

References

[1] Y. Okamoto, Bull. Chem. Soc. Jpn. 87 (2013) 20-58.

[2] S.T. Oyama, T. Gott, H. Zhao, Y.K. Lee, Catal. Today 143 (2009) 94-107.

[3] R. Prins, M.E. Bussell, Catal. Lett. 142 (2012) 1413-1436.

[4] P. Liu, J.A. Rodriguez, T. Asakura, J. Gomes, K. Nakamura, J. Phys. Chem. B 109 (2005) 4575-4583.

[5] W.R.A.M. Robinson, J.N.M.van Gestel, T.I. S. Koranyi, Eijsbouts, A.M. van der Kraan, J.A.R. van Veen, V.H.J. de Beer, J. Catal. 161, (1996) 539-550.

[6] C. Stinner, Z. Tang, M. Haouas, Th.Weber, R. Prins, J. Catal. 208 (2002) 456-466.

[7] S.T. Oyama, X.Wang, Y.K. Lee, K. Bando, F.G. Requejo, J. Catal. 210 (2002) 207-217.

[8] S.J. Sawhill, D.C. Philips, M.E. Bussell, J. Catal. 215 (2003) 208-219.

[9] T.I. Korányi, Appl. Catal. A: Gen. 239 (2003) 253-267.

[10] A. Wang, L. Ruan, Y. Teng, X. Li, M. Lu, J. Rena, Y. Wang, Y. Hu, J. Catal. 229 (2005) 314-321.

[11] S.J. Sawhil, K.A. Layman, D.R. Van Wyk, M.H. Engelhard, C. Wang, M.E. Bussell, J. Catal. 231 (2005) 300-313.

[12] S. Yang, C. Liang, R. Prins, J. Catal. 237 (2006) 118-130.

[13] Y.K. Lee, S.T. Oyama, Appl. Catal. A: Gen. 322 (2007) 191-204.

[14] S.T. Oyama, Y.K. Lee, J. Catal. 258 (2008) 393-400.

[15] E. Muthuswamy, G.H.L. Savithra, S.L. Brock, ACS Nano 5 (2011) 2402-2411.

[16] S.T. Oyama, J. Catal. 216 (2003) 343-352.

[17] J.A. Rodriguez, J.Y. Kim, J.C. Hanson, S.J. Sawhill, M.E. Bussell, J. Phys. Chem. B, 107 (2003) 6276-6285.

[18] P. Clark, X. Wang, S.T. Oyama, J. Catal. 207 (2002) 256-265.

[19] S.J. Sawhill, D.C. Phillips, M.E. Bussell, J. Catal. 215 (2003) 208-219.

[20] P.A. Clark, S.T. Oyama, J. Catal. 218 (2003) 78-87.

[21] A. Montesinos-Castellanos, T.A. Zepeda, B. Pawelec, J.L.G. Fierro, J.A. de los Reyes, Chem. Mater. 19 (2007) 5627-5636.

[22] A. Montesinos-Castellanos, T.A. Zepeda, B. Pawelec, E. Lima, J.L.G. Fierro, A. Olivas, J.A. de los Reyes H., Appl. Catal. A: Gen. 334 (2008) 330-338.

[23] Y. Kanda, C. Temma, K. Nakata, M. Sugioka, Y. Uemichi, Appl. Catal. A: Gen. 386 (2010) 171-178.

[24] Y. Kanda, K. Nakata, C. Temma, M. Sugioka, Y. Uemichi, J. Jpn.

Petrol. Inst. 55 (2012) 108-119.

[25] Y. Kanda, T. Ichiki, S. Kayaoka, A. Sawada, M. Sugioka, Y. Uemichi, Chem. Lett. 42 (2013) 404-406.

[26] Y. Kanda, C. Temma, A. Sawada, M. Sugioka, Y. Uemichi, Appl. Catal. A: Gen. 475 (2014) 410-419.

[27] Y. Kanda, Y. Uemichi, J. Jpn. Petrol. Inst. 58 (2015) 20-32.

[28] J.R. Hayes, R.H. Bowker, A.F. Gaudette, M.C. Smith, C.E. Moak, C.Y. Nam, T.K. Pratum, M.E. Bussell, J. Catal. 276 (2010) 249-258.

[29] V. Teixeira da Silva, L.A. Sousa, R.M. Amorim, L. Andrini, S.J.A. Figueroa, F.G. Requejo, F.C. Vicentini, J. Catal., 279 (2011) 88-102.

[30] A. Sawada, Y. Kanda, M. Sugioka, Y. Uemichi, Catal. Commun., 56 (2014) 60-64.

[31] R.H. Bowker, M.C. Smith, B.A. Carrillo, M.E. Bussell, Top. Catal., 55 (2012) 999.

[32] J.A. Cecilia, A. Infantes-Molina, E. Rodríguez-Castellón, A. Jiménez-López, J. Phys. Chem. C, 113 (2009) 17032–17044.

[33] E.L. Muetterties, J.C. Sauer, J. Am. Chem. Soc., 96 (1974) 3410–3415.

[34] A.E. Henkes, R.E. Schaak, Chem. Mater. 19 (2007) 4234-4242.

[35] K.S. Cho, H.R. Seo, Y.K. Lee, Catal. Commun. 12 (2011) 470-474.

[36] H. Song, M. Dai, H. Song, X. Wan, X. Xu, C. Zhang, H. Wang, Catal. Commun. 43 (2014) 151-154.

[37] H. Song, M. Dai, H.L. Song, X. Wan, X.W. Xu, Z.S. Jin, J. Mol. Catal. A: Chem. 385 (2014) 149-159.

[38] C.P. Hwang, C.T. Yeh, Q. Zhu, Catal. Today 51 (1999) 93-101.

[39] J.P. Contour, G. Mouvier, J. Catal. 48 (1977) 217-228.

[40] Y. Okamoto, N. Ishida, T. Imanaka, S. Teranishi, J. Catal. 58 (1979) 82-94.

[41] C.P. Booker, J.T. Keiser, J. Phys. Chem. 93 (1989) 1532-1536.

[42] P. Castillo-Villalón, J. Ramírez, F. Maugé, J. Catal. 260 (2008) 65-74.

[43] L. Li, L.L. Wang, D.D. Johnson, Z. Zhang, S.I. Sanchez, J.H. Kang, R.G. Nuzzo, Q. Wang, A.I. Frenkel, J. Li, J. Ciston, E.A. Stach, J.C. Yang, J. Am. Chem. Soc. 135 (2013) 13062-13072.

[44] S.I. Sanchez, M.W. Small, E.S. Bozin, J.G. Wen, J.M. Zuo, R.G. Nuzzo, ACS Nano, 7 (2013) 1542-1557.

Captions

Figure 1 TPR profiles of P(T)/Rh/Al_2O_3 catalyst recorded by TCD and FID.

Figure 2 XRD patterns of P(T)/Rh/Al_2O_3 catalyst reduced at 450 °C–650 °C.

Figure 3 XRD patterns of HL-P(T)/Rh/Al_2O_3 catalyst reduced at 350 °C–650 °C.

Figure 4 XPS spectra of P(T)/Rh/Al_2O_3 catalyst reduced at 450 °C–650 °C.

Figure 5 Relationship between the reduction temperature and CO uptake of P(T)/Rh/Al_2O_3 catalyst.

Figure 6 TEM images of P(T)/Rh/Al_2O_3 catalyst (A) before and after reduction at (B) 450 °C, (C) 550°C, and (D) 650 °C.

Figure 7 Particle size distribution of P(T)/Rh/Al_2O_3 catalyst (A) before and after reduction at (B) 450 °C, (C) 550°C, and (D) 650 °C.

Figure 8 HDS of thiophene over P(T)/Rh/Al_2O_3 catalyst after reduction at 450-700 °C.

Table 1 CO uptake and average particle size calculated from TEM images of P(T)/Rh/Al_2O_3 catalyst before and after reduction.

Reduction temperature (°C)	CO uptake (μmol g^{-1})	Average particle size (nm)
Before reduction	-	0.97
450	91.6	1.18
500	142.3	-
550	171.5	1.25
600	188.1	-
650	178.7	1.31
700	165.7	-

Table 2 HDS properties of P(T)/Rh/Al_2O_3 catalyst. Reaction conditions: H_2/C_4H_4S = 30, total pressure = 0.1 MPa.

Reduction temperature (°C)	W/F (g h mol^{-1})	Thiophene conversion (%)	k_{HDS} (mmol g^{-1} h^{-1})	TOF (h^{-1})	Selectivity of HDS products (%)			
					C_1-C_3[a]	Butanes	Butenes	THT[b]
450	37.9	27.4	8.5	79.0	0.6	37.8	60.5	1.0
500	37.9	47.9	17.3	88.9	0.7	46.3	51.8	1.2
550	37.9	63.0	26.2	96.7	0.7	50.6	47.7	1.0
600	37.9	72.5	34.0	101.6	0.6	53.1	45.4	0.9
650	37.9	76.7	38.5	113.2	0.4	52.5	46.2	0.9
700	37.9	70.9	32.7	112.9	0.4	41.4	56.6	1.6
600	26.5	52.9	28.4	106.1	0.9	42.3	55.0	1.7

a C_1-C_3 hydrocarbons

b Tetrahydrothiophene

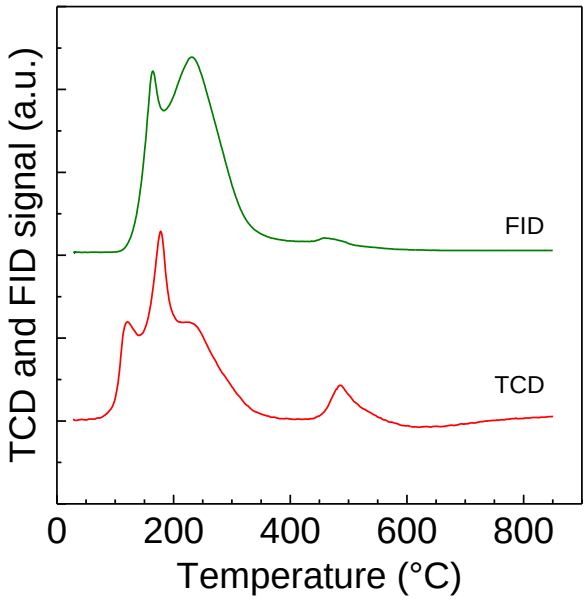

Fig. 1

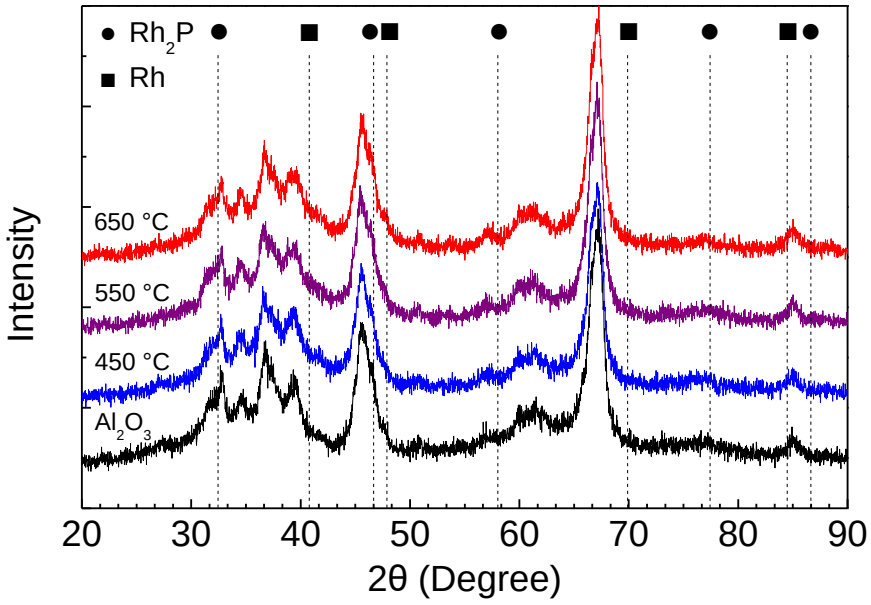
● Rh2P
■ Rh
650 °C
550 °C
450 °C
Al2O3
Intensity
20
30
40
50
60
70
80
90
2θ (Degree)

Fig. 2

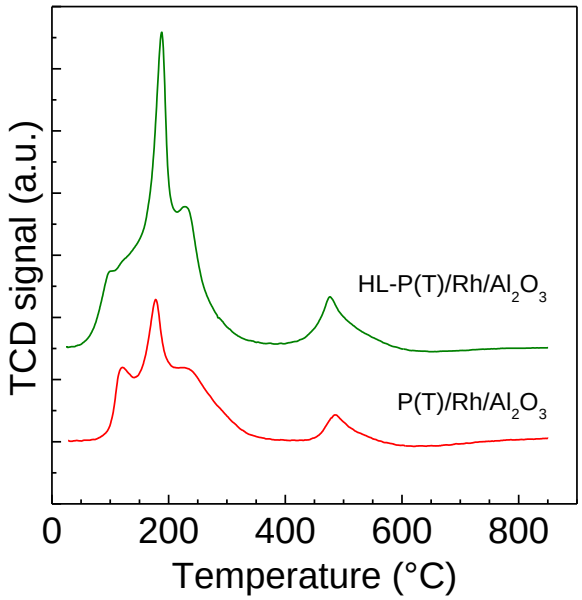
TCD signal (a.u.)
HL-P(T)/Rh/Al2O3
P(T)/Rh/Al2O3
0
200
400
600
800
Temperature (°C)

Fig. 3

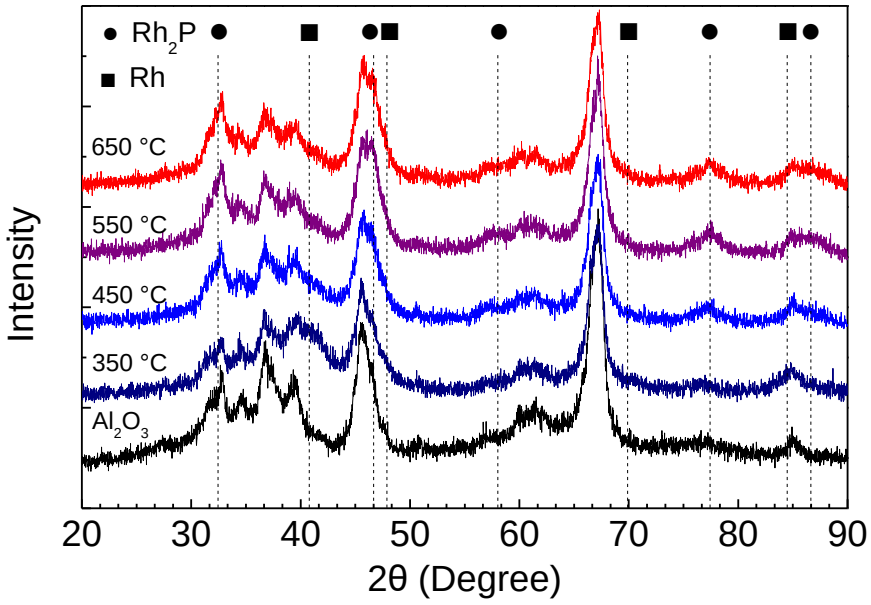
● Rh2P
■ Rh
650 °C
550 °C
450 °C
350 °C
Al2O3
Intensity
20
30
40
50
60
70
80
90
2θ (Degree)

Fig. 4

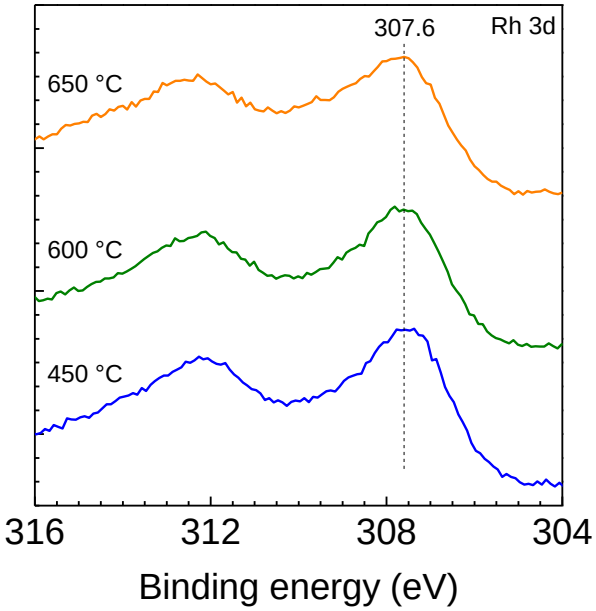
307.6
Rh 3d
650 °C
600 °C
450 °C
316
312
308
304
Binding energy (eV)

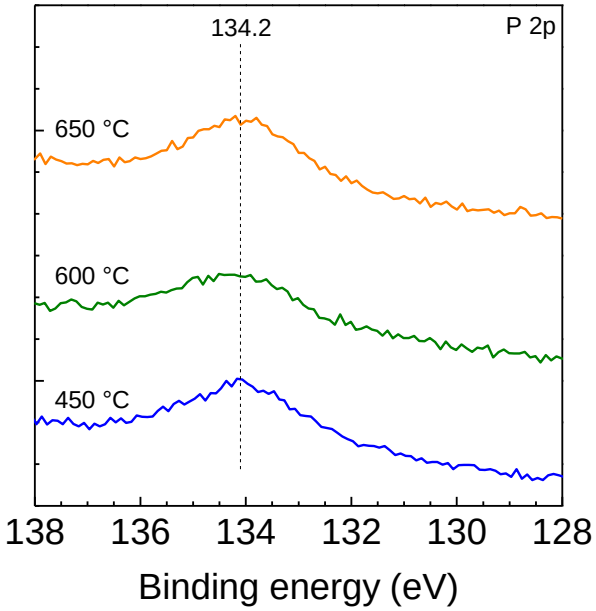
134.2
P 2p
650 °C
600 °C
450 °C
138
136
134
132
130
128
Binding energy (eV)

Fig. 5

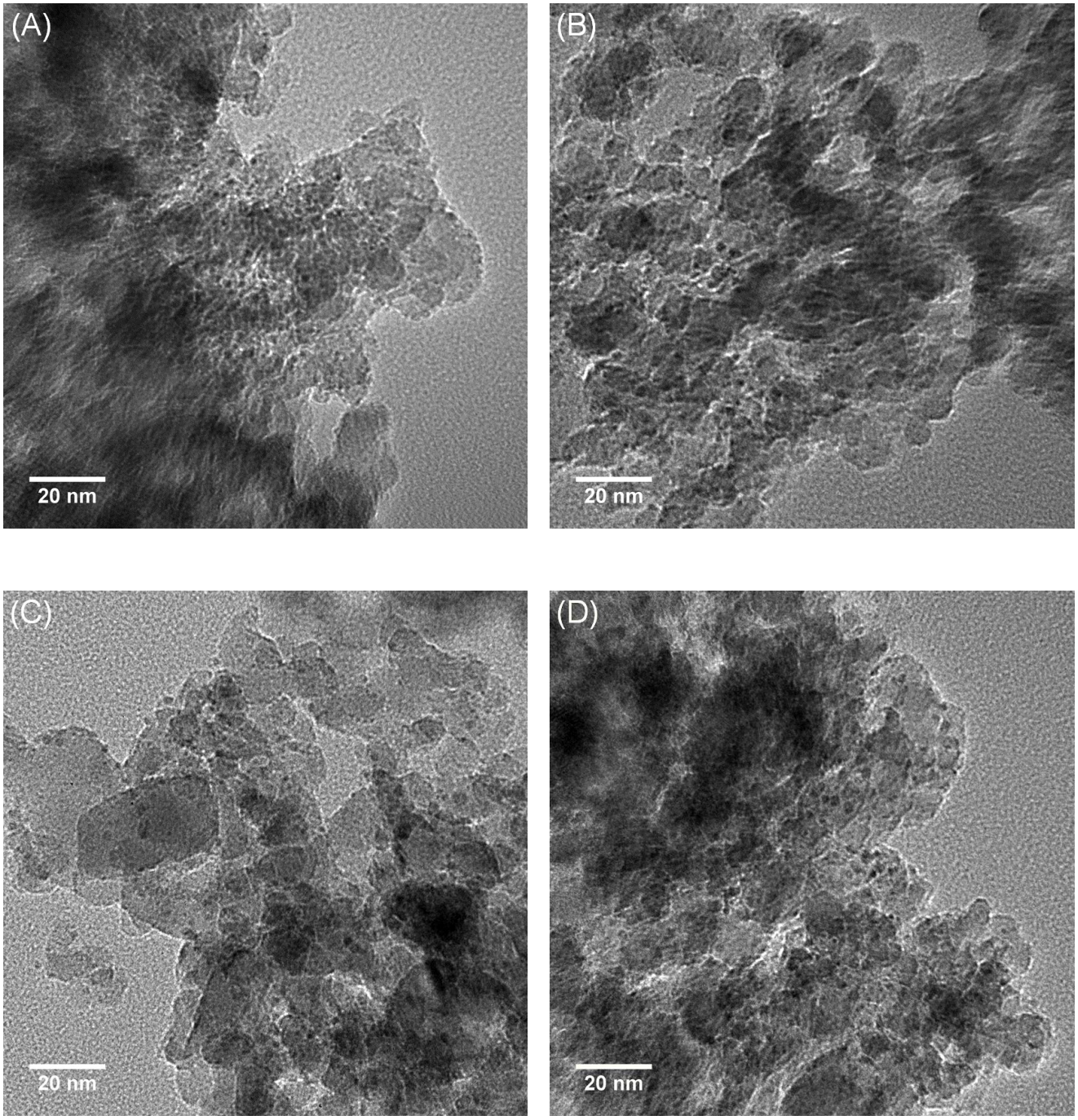

Fig. 6

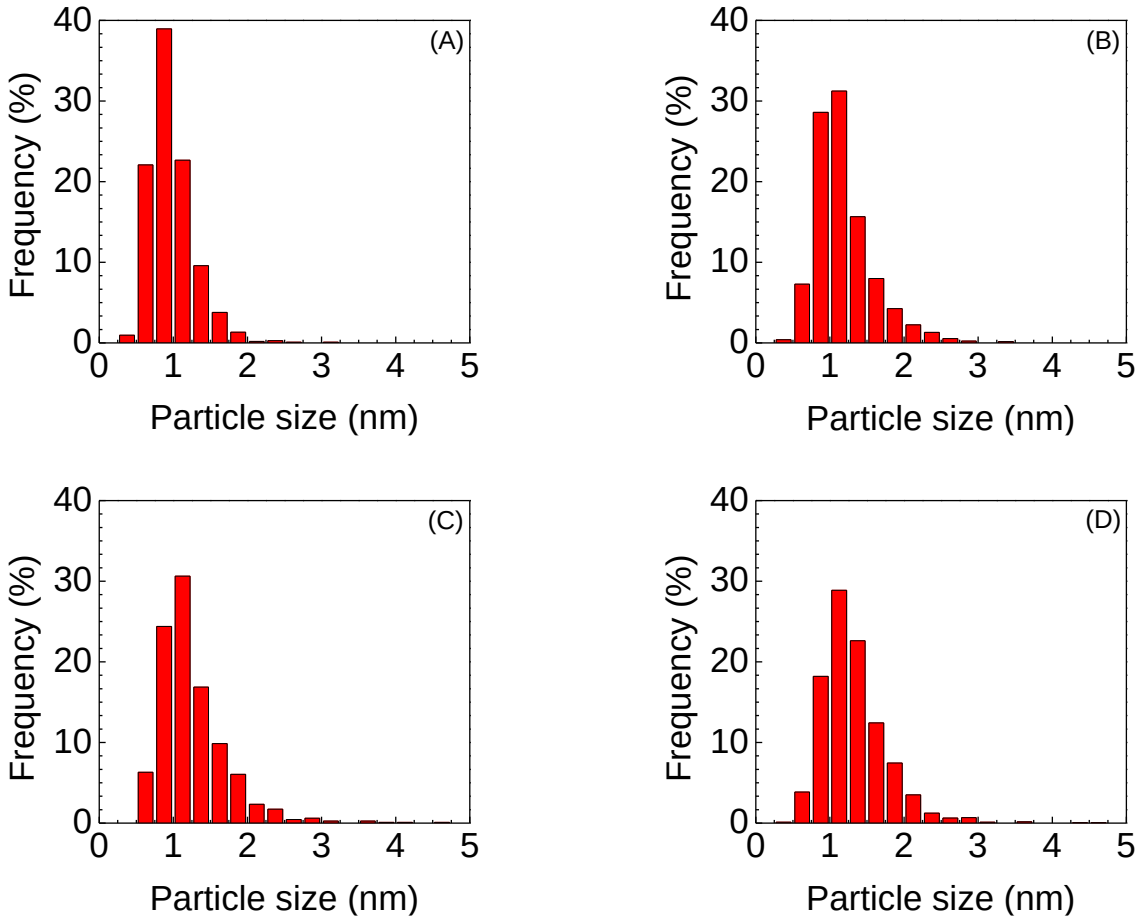

Fig. 7

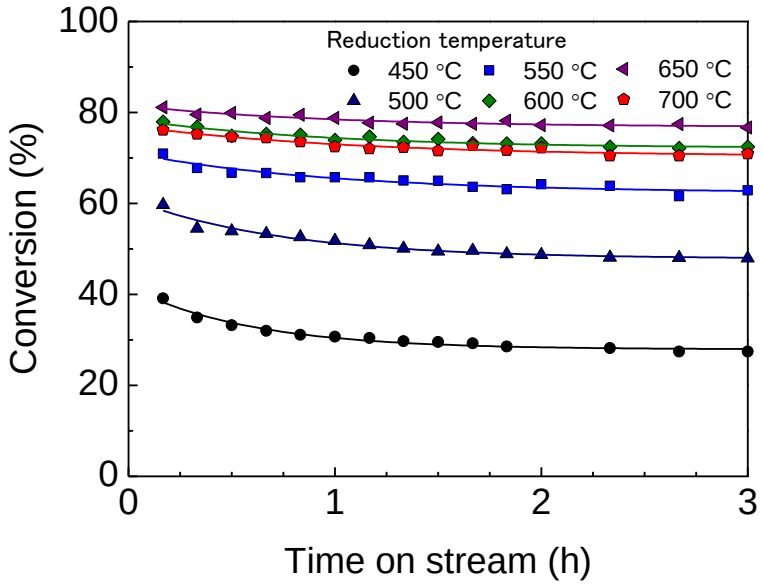
Reduction temperature
450 °C
550 °C
650 °C
500 °C
600 °C
700 °C
Conversion (%)
Time on stream (h)
0
20
40
60
80
100
0
1
2
3

Fig. 8

Graphical abstract